한국지반공학회논문집 제19권 4호 2003년 8월 pp. 277 ~ 286

Large Deformation Formulation of a Hypoelasto-plastic Constitutive Model for Soils

흙의 속도형식 탄소성구성모델에 대한 대변형도 정식화

Oh, Se-Boong[*1] 오 세 붕
Lee, Seung-Hyun[*2] 이 승 현
Kwon, Oh-Kyun[*3] 권 오 균

요 지

미소변형에서 대변형에 이르는 전변형도 영역의 거동을 모델하기 위하여 비등방 경화규칙과 전응력개념에 의거한 구성관계를 이용하였다. 이러한 구성관계는 ABAQUS 코드에 구현되었으며 대변형해석시 정확도와 수렴속도를 확보하도록 하였다. 이 정식화는 Jaumann 응력속도에 의거한 유한 변형도 소성론, 내재적 응력적분, 일관된 접선계수를 포함한다. ABAQUS를 이용한 대변형해석을 통하여 알고리즘의 정확도 및 수렴도 해석을 할 수 있었다.

Abstract

A constitutive equation was implemented in order to model the behavior in overall ranges from small to large strains, which is based on anisotropic hardening rule and total stress concept. The constitutive model was implemented in ABAQUS code in which large deformation analysis can be performed accurately and efficiently. The formulation includes (1) finite strain plasticity on the basis of Jaumann stress rate, (2) implicit stress integration and (3) consistent tangent moduli. A large deformation analysis was performed with the constitutive model using ABAQUS program. In the analysis of an actual embankment, it was found that the proposed model was formulated accurately and efficiently.

Keywords : Anisotropic hardening rule, Finite strain plasticity, Hypoelasticity, Large strains, Stress integration

1. Introduction

As for the stress-strain relationship of geomaterials, the actual behavior is nonlinear in the overall range from small to large strains (10^{-4} to 10%) and is also dependent on various and complicated factors. The important portion of the overall relationship depends on each problem and hence it is required to acquire and model such an overall behavior. In experiments it is difficult to measure small strains accurately but in analyses the formulation and analysis of large deformations are complicated. This study is focused on the latter part.

On the viewpoint of nonlinear continuum mechanics, hypoelasticity is frequently used in practice while it limits its applicability to small stretching and the isotropy of elasticity (Hughes 1984). Then an objective rate, or Jaumann stress rate is commonly used in geomaterials (Hughes 1984, Lush et al. 1989, Simo and Hughes 1998).

The rate form of elasto-plastic constitutive equations

*1 Member, Associate Prof, Dept. of Civil Eng., Yeungnam Univ. (sebungoh@yu.ac.kr)
*2 Member, Assistant Prof., Dept. of Civil Eng., Sunmoon Univ.
*3 Member, Associate Prof., Dept. of Civil Eng., Keimyung Univ.

is required to integrate numerically. The implicit integration method has been regarded as the most appropriate scheme to hold the accuracy while the tangential stress-strain modulus should be consistent with the linearization in order to conserve the quadratic rate of convergence (Ortiz and Popov 1985, Simo and Taylor 1985, Dodds 1987, Crisfield 1991, Oh and Lee 2001).

As for the material behavior, anisotropic hardening models in the context of elasto-plasticity can capture successfully the actual behavior of soils (Dafalias 1981, Mroz et al. 1981, Borja and Amies 1994). The anisotropy in hardening description tried to model hysterisis and cyclic nonlinearity but is also useful to simulate general nonlinearity under overconsolidated or K_0 condition (Dafalias, 1981, Lee and Oh, 1995). An elasto-plastic constitutive model based on anisotropic hardening rule and total stress concept was proposed to model the stress-strain behavior from small to large strains (10^{-4} to 10%) (Oh 2003). In order to solve the stability problem of soft clays the constitutive model is based on (1) elstoplasticity and total stress concept, (2) the generalized isotropic hardening description with a simple hardening equation and (3) the evaluation of stress-strain relationship from undrained triaxial tests and site investigation data.

In this study implicit stress integration of that model is formulated based on nonlinear continuum mechanics for large deformation analysis. Tangent modulus is also formulated from the stress integration procedure and coded into a user subroutine of ABAQUS code (HK & S 2001). An example of embankment on soft clays verifies accuracy and convergence rate of the algorithm and evaluates plastic deformations under reverse loading.

2. Constitutive Equations for Finite Deformation Plasticity

Based on finite deformation plasticity theory, the constitutive equation based on hypoelasticity can be written as follows (Hughes, 1984, Lush, 1990):

$$\overset{\nabla}{\mathbf{T}} = \mathbf{C}^e : \left(\mathbf{D} - \mathbf{D}^p\right) \tag{1}$$

where

$\overset{\nabla}{\mathbf{T}} \equiv \dot{\mathbf{T}} - \mathbf{WT} + \mathbf{TW}$	Jaumann rate of Cauchy stress $\mathbf{T}$
$\dot{\mathbf{T}}$	material time derivative of Cauchy stress $\mathbf{T}$
$\mathbf{C}^e = 2G\mathbf{I} + (K - \frac{2}{3}G)\mathbf{1}\otimes\mathbf{1}$	isotropic elasticity tensor
K, G	elastic bulk and shear moduli
$\mathbf{1} = \delta_{ij}$	Kronecker delta tensor
$\mathbf{I}$	fourth order identity tensor
$\mathbf{L} \equiv \text{grad}\ \mathbf{v}$	spatial gradient of velocity $\mathbf{v}$
$\mathbf{D} \equiv \text{sym}\ (\mathbf{L})$ d	eformation rate tensor
$\mathbf{W} \equiv \text{skew}\ (\mathbf{L})$	spin tensor

Equation (1) is motivated by infinitesimal plasticity theory with a decomposition of deformation rate tensor into elastic and plastic parts, $\mathbf{D} = \mathbf{D}^e + \mathbf{D}^p$. On the viewpoint of elasticity, this equation is objectionable on fundamental grounds of hyperelasticity but frequently used in practice. It also limits its applicability to the small stretching and the isotropy of elasticity (Hughes 1984, Simo and Hughes 1998).

A spatial tensor field is said to transform objectively under superposed rigid body motions if it transforms according to the standard rules of tensor analysis. However, assuming that the Cauchy stress tensor is objective, its material time derivative is not objective (Simo and Hughes 1998, Hughes 1984). Accordingly an objective rate is required and Jaumann stress rate is commonly used in geomaterials.

The flow rule for $\mathbf{D}^p$ is described as

$$\mathbf{D}^p = \dot{\gamma}\mathbf{N} \tag{2}$$

where $\dot{\gamma}$ is scalar consistency parameter related to the magnitude of $\mathbf{D}^p$ and the direction of plastic flow is associated with the normal of yield surface

$$\mathbf{N} = \frac{\partial f}{\partial \mathbf{T}} \tag{3}$$

Hardening rule for internal variable r is related to the invariant of plastic strain

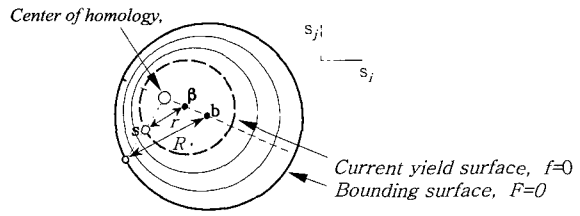

Fig. 1. Bounding and yield surfaces in the deviatoric stress field

$$\dot{r} = h(r)\dot{\tilde{\varepsilon}}^p \tag{4}$$

where $\dot{\tilde{\varepsilon}}^p \equiv \sqrt{2/3}\left\|\mathrm{dev}(\mathbf{D}^p)\right\|$.

A constitutive model was proposed by Oh (2003), which includes bounding and yield surfaces as follows (Fig. 1)

$$F = (\mathbf{s}^* - \mathbf{b}) : (\mathbf{s}^* - \mathbf{b}) - R^2 = 0 \tag{5}$$

$$f = (\mathbf{s} - \boldsymbol{\beta}) : (\mathbf{s} - \boldsymbol{\beta}) - r^2 = 0 \tag{6}$$

Stress tensors are decomposed into volumetric and deviatoric terms as $\mathbf{T} = p\mathbf{1} + \mathbf{s}$.

In equations (5) and (6), $\mathbf{b}$ and $\boldsymbol{\beta}$ are deviatoric terms of center stresses for bounding and yield surfaces. Furthermore, $\mathbf{s}^*$ is a mapping stress onto the bounding surface. The variable r is the radius of yield surface and R is that of bounding surface.

Assuming that the deviatoric part of plastic strain is dependent on the radius of the yield surface, the hardening function of yield surfaces is defined as

$$\tilde{\varepsilon}^p = a\frac{(r/R)^b}{(1-r/R)^c} \tag{7}$$

Three parameters a, b and c are required to describe the anisotropic hardening rule. $\tilde{\varepsilon}^p$ is a strain measure of integrating $\dot{\tilde{\varepsilon}}^p$ over a loading process. Equation (7) is a flexible function to describe the stress-plastic strain behavior of geomaterials, which represents a form of hyperbolic stress-strain curve when b=2 and c=1and Ramberg-Osgood curve when c=0 (Oh 2003). The function $h(r)$ in equation (4) is derived from equation (7)

$$h(r) = \frac{R(1-r/R)^{c+1}}{ab(1-r/R)(r/R)^{b-1} + ac(r/R)^b} \tag{8}$$

For the skew-symmetric spin tensor, $\mathbf{W} = -\mathbf{W}^T$ and a rotation tensor $\mathbf{Q}(t)$ is generated at $t \in [t_n, t_{n+1}]$ by solving

$$\dot{\mathbf{Q}} = \mathbf{W}\mathbf{Q} \tag{9}$$

$$\mathbf{Q}|_{t=t_n} = \mathbf{1} \tag{10}$$

When transformed by $\mathbf{Q}$, Cauchy stress or a symmetric second order tensor takes on a simple form

$$\overline{\mathbf{T}} = \mathbf{Q}^T\mathbf{T}\mathbf{Q} \tag{11}$$

Then its material time derivative is derived as (Hughes, 1984, Lush et al, 1989)

$$\dot{\overline{\mathbf{T}}} = \mathbf{Q}^T \overset{\nabla}{\mathbf{T}} \mathbf{Q} \tag{12}$$

This transformation makes the formulation and implementation of stress integrations simple.

Assuming the isotropy of $\mathbf{C}^e$, equations from (1) to (4) are rewritten as follows

$$\dot{\overline{\mathbf{T}}} = \mathbf{C}^e : (\overline{\mathbf{D}} - \overline{\mathbf{D}}^p) \tag{13}$$

$$\overline{\mathbf{D}}^p = \dot{\gamma}\overline{\mathbf{N}} \tag{14}$$

$$\overline{\mathbf{N}} = \frac{\partial f}{\partial \overline{\mathbf{T}}} \tag{15}$$

$$\dot{r} = h(r)\dot{\tilde{\varepsilon}}^p \tag{16}$$

3. Implicit Stress Integration

The rate form of constitutive equation (13) should be integrated over an interval $[t_n, t_{n+1}]$

$$\overline{\mathbf{T}}_{n+1} = \overline{\mathbf{T}}_n + \int_{t_n}^{t_{n+1}} \mathbf{C}^e : (\overline{\mathbf{D}} - \overline{\mathbf{D}}^p)dt \tag{17}$$

where the previous time step t_n defines converged configuration and t_{n+1} the subsequent configuration under current iteration. Subscripts n and n+1 on variables indicate the time step t_n and t_{n+1} at which the variables

are evaluated.

Using $\overline{\mathbf{T}}_n = \mathbf{T}_n$ from equations (10) and (11) and also assuming that $\mathbf{C}^e$ is constant over a time increment, then

$$\overline{\mathbf{T}}_{n+1} = \overline{\mathbf{T}}^{tr} - \mathbf{C}^e : \int_{t_n}^{t_{n+1}} \overline{\mathbf{D}}^p dt \tag{18}$$

where prescribed trial stress tensor is defined as

$$\overline{\mathbf{T}}^{tr} = \mathbf{T}_n + \mathbf{C}^e : \int_{t_n}^{t_{n+1}} \overline{\mathbf{D}} dt \tag{19}$$

The right-hand side of equation (19) is computed from converged variables at t_n and inputs at $t \in [t_n, t_{n+1}]$.

The plastic deformation rate in equation (18) is integrated by the generalized trapezoidal rule as follows (Ortiz and Popov 1985)

$$\int_{t_n}^{t_{n+1}} \overline{\mathbf{D}}^p dt \cong \left\{(1-\alpha)\left(\overline{\mathbf{D}}^p\right)_n + \alpha\left(\overline{\mathbf{D}}^p\right)_{n+1}\right\}\Delta t \tag{20}$$

$\left(\overline{\mathbf{D}}^p\right)_n$ and $\left(\overline{\mathbf{D}}^p\right)_{n+1}$ are transformed rates of plastic deformation at each time step and α is trapezoidal parameter. If $\alpha = 0$, the stresses are integrated by an explicit forward Euler method. For $\alpha = 1$, the backward Euler method or the closest point projection algorithm is obtained (Crisfield 1991). According to the backward Euler method, equation (18) becomes

$$\overline{\mathbf{T}}_{n+1} \cong \overline{\mathbf{T}}^{tr} - \mathbf{C}^e : \Delta t\left(\overline{\mathbf{D}}^p\right)_{n+1} \tag{21}$$

As $\left(\overline{\mathbf{D}}^p\right)_{n+1}$ is dependent on the unknown $\overline{\mathbf{T}}_{n+1}$, the stress integration of equation (21) should be implicitly performed by iterative procedures. In this study, the constitutive model is implemented in a displacement based finite element code, ABAQUS (version 6.2.1, 2001) by writing a 'user material' subroutine (UMAT). It is required to fit inputs and outputs of this formulation into the constitutive routine of ABAQUS.

In the first place, equation (21) is described using Cauchy stresses (Lush et al., 1989, Lush, 1990)

$$\mathbf{Q}_{n+1}^T \mathbf{T}_{n+1} \mathbf{Q}_{n+1} = \overline{\mathbf{T}}^{tr} - \mathbf{C}^e : \left\{\mathbf{Q}_{n+1}^T \Delta t\left(\mathbf{D}^p\right)_{n+1} \mathbf{Q}_{n+1}\right\} \tag{22}$$

Accordingly

$$\mathbf{T}_{n+1} = \mathbf{T}^{tr} - \mathbf{C}^e : \left\{\Delta t\left(\mathbf{D}^p\right)_{n+1}\right\} \tag{23}$$

where another trial stress is defined as

$$\mathbf{T}^{tr} \equiv \mathbf{Q}_{n+1} \overline{\mathbf{T}}^{tr} \mathbf{Q}_{n+1}^T = \mathbf{T}_n^Q + \mathbf{C}^e : \Delta \mathbf{E}_{n+1}^Q \tag{24}$$

$$\mathbf{T}_n^Q \equiv \mathbf{Q}_{n+1} \mathbf{T}_n \mathbf{Q}_{n+1}^T \tag{25}$$

$$\Delta \mathbf{E}_{n+1}^Q = \mathbf{Q}_{n+1} \left\{\int_{t_n}^{t_{n+1}} \overline{\mathbf{D}} dt\right\} \mathbf{Q}_{n+1}^T \tag{26}$$

ABAQUS provides $\mathbf{T}_n^Q$ and $\Delta \mathbf{E}_{n+1}^Q$ of equations (25) and (26) in UMAT for each integration point and calculates $\mathbf{Q}_{n+1}$ by Hughes-Winget algorithm (1980). Consequently $\mathbf{T}^{tr}$ in equation (24) can be readily obtained. After integration Cauchy stresses and internal variables are saved as outputs.

According to the flow rule equation (23) is derived as

$$\mathbf{T}_{n+1} = \mathbf{T}^{tr} - \mathbf{C}^e : \Delta\gamma \mathbf{N}_{n+1} \tag{27}$$

where $\Delta\gamma \equiv \dot{\gamma}\Delta t$. Stress tensors are decomposed as $\mathbf{T}_{n+1} = p\mathbf{1} + \mathbf{s}$ and the trial stress in equation (23) is decomposed as

$$p^{tr} \equiv \tfrac{1}{3}\mathrm{tr}(\mathbf{T}^{tr}), \mathbf{s}^{tr} \equiv \mathbf{T}^{tr} - \tfrac{1}{3}\mathrm{tr}(\mathbf{T}^{tr}) \tag{28}$$

Accordingly equation (27) is written as

$$\mathbf{s} = \mathbf{s}^{tr} - 2G\Delta\gamma \mathbf{N}_{n+1} \tag{29}$$

The integration of internal variables is obtained by the backward Euler method as follows

$$r_{n+1} = r_n + \sqrt{\tfrac{2}{3}} h(r_{n+1}) \Delta\gamma \left\|\mathbf{N}_{n+1}\right\| \tag{30}$$

However, the constitutive model in this study has a hardening function which is integrable explicitly. The integration of plastic strain rate $\dot{\tilde{\varepsilon}}^p$ can be interpreted as

$$\tilde{\varepsilon}_{n+1}^p = \sqrt{\tfrac{2}{3}} \left\|\mathbf{e}_{n+1}^p\right\| = \psi(r_{n+1}) \tag{31}$$

Table 1. Algorithm solving $\mathbf{R}(\mathbf{X}_{n+1}) = \mathbf{0}$

1.	Initialize $m = 0, \mathbf{X}_{n+1}^{m} = \mathbf{0}$
2.	Compute $\mathbf{R}^{m} = \mathbf{R}(\mathbf{X}_{n+1}^{m})$
3.	If $\|\mathbf{R}^{m}\| / \|\mathbf{R}^{0}\|$ < Tolerance, return; else
4.	Update $\mathbf{X}_{n+1}^{m+1} = \mathbf{X}_{n+1}^{m} - \Delta\mathbf{X}^{m}$ such that $\mathbf{R}'(\mathbf{U}_{n+1}^{m})\Delta\mathbf{X}^{m} = \mathbf{R}^{m}$
5.	$m \leftarrow m+1$ and go to 2

where

$$\mathbf{e}_{n+1}^{p} = \mathbf{e}_{n}^{p} + \Delta\gamma\mathbf{N}_{n+1}, \quad \psi(r) = a\frac{(r/R)^{b}}{(1-r/R)^{c}} \tag{32}$$

For simplicity let $\mathbf{e}^{p} \equiv \mathbf{e}_{n+1}^{p}$ and $r \equiv r_{n+1}$. Variables without subscripts are generated at t_{n+1}.

Therefore, equation (29) is solved implicitly with equations (6) and (31). Let a residual be defined as $\mathbf{R} = \{\mathbf{r}_1^{T}, r_2, r_3\}^{T}$ for variable vector $\mathbf{X} = \{\mathbf{s}^{T}, \Delta\gamma, r\}^{T}$. Then,

$$\mathbf{r}_1 = \mathbf{s} - \mathbf{s}^{tr} + 2G\Delta\gamma\mathbf{N} \tag{33}$$

$$r_2 = \sqrt{2/3}\|\mathbf{e}^{p}\| - \psi(r) \tag{34}$$

$$r_3 = (\mathbf{s}-\boldsymbol{\beta}):(\mathbf{s}-\boldsymbol{\beta}) - r^{2} \tag{35}$$

The stress integration is then a problem for solving the following nonlinear system.

$$\mathbf{R}(\mathbf{X}_{n+1}) = \mathbf{0} \tag{36}$$

where n+1 is the current step number. Thus a linearization of equation (36) is required and iterations are performed over

$$\mathbf{R}'(\mathbf{X}_{n+1}^{m})\Delta\mathbf{X}^{m} = \mathbf{R}^{m}, \quad \mathbf{X}_{n+1}^{m+1} = \mathbf{X}_{n+1}^{m} - \Delta\mathbf{X}^{m} \tag{37}$$

where m is the iteration count under stress integration. The solution procedure is described in Table 1. See Appendix I for details of equation (37).

4. Consistent Tangent Moduli

In order to maintain the quadratic convergence of implicit finite element solver, the tangent modulus must be *consistent* with the numerical method employed to integrate the constitutive equations (Simo and Taylor 1985). Consistency implies that the stress increment calculated by the tangent modulus operating on the strain increment matches the stress increment calculated by the integration procedure to the first order (Dodds 1987). The consistent tangent modulus is then derived from the differentiation of stress integration functions with appropriate strain measure

$$\mathbf{C}_{n+1}^{k} = \frac{\partial\mathbf{T}_{n+1}^{k}}{\partial\Delta\mathbf{E}_{n+1}^{Q}} = \mathbf{1}\otimes\frac{\partial p_{n+1}^{k}}{\partial\Delta\mathbf{E}_{n+1}^{Q}} + \frac{\partial\mathbf{s}_{n+1}^{k}}{\partial\Delta\mathbf{E}_{n+1}^{Q}} \tag{38}$$

where k is global iteration count at $t\in[t_n, t_{n+1}]$

Let $x \equiv x_{n+1}^{k}$ and $x' \equiv \partial x_{n+1}^{k} / \partial\,\Delta\mathbf{E}_{n+1}^{Q}$ and then for equation (38)

$$p' = (p^{tr})' \tag{39}$$

$$\mathbf{s}' = (\mathbf{s}^{tr})' - 2G\mathbf{N}\otimes\Delta\gamma' - 2G\Delta\gamma\mathbf{N}' \tag{40}$$

From equation (24), $(p^{tr})' = K\mathbf{1}$, $(\mathbf{s}^{tr})' = 2G(\mathbf{I} - \frac{1}{3}\mathbf{1}\otimes\mathbf{1})$, equation (38) is derived as

$$\mathbf{C}_{n+1}^{k} = K\mathbf{1}\otimes\mathbf{1} + \frac{\partial\mathbf{s}_{n+1}^{k}}{\partial\Delta\mathbf{E}_{n+1}^{Q}} \tag{41}$$

Accordingly, $\partial\mathbf{s}_{n+1}^{k} / \partial\Delta\mathbf{E}_{n+1}^{Q}$ is required to be evaluated.

From equation (A1.1) in Appendix I,

$$\mathbf{N}' = 2(\mathbf{s}' - \boldsymbol{\beta}') \tag{42}$$

and

$$\boldsymbol{\beta}' = \boldsymbol{\beta}_{,r}\otimes r' \tag{43}$$

where $f_{,x} \equiv \partial f / \partial x$

From equation (31),

$$\sqrt{\tfrac{2}{3}}\frac{\mathbf{e}^{p}}{\|\mathbf{e}^{p}\|}:\{\Delta\gamma'\mathbf{N} + \Delta\gamma\mathbf{N}'\} = \psi_{,r}\, r' \tag{44}$$

and from equation (6)

$$\mathbf{N}:(\mathbf{s}' - \boldsymbol{\beta}') + f_{,r}\, r' = 0 \tag{45}$$

Table 2. Algorithm coded in UMAT

1.	Read $\mathbf{T}_n^Q$, $\Delta\mathbf{E}_{n+1}^Q$ and state variables from INPUT.
2.	Calculate $\mathbf{T}^{tr}$ $\mathbf{T}^{tr} = \mathbf{T}_n^Q + \mathbf{C}^e : \Delta\mathbf{E}_{n+1}^Q$
3.	Check reverse loading if $\mathbf{N} : (\mathbf{C}^e : \Delta\mathbf{E}_{n+1}^Q) < 0$ then Reset state variables $r_n = 0$, $\mathbf{e}_n^p = \mathbf{0}$ and $\boldsymbol{\beta}_n = \mathbf{0}$ end if
4.	Integrate stress by iteration such that $\mathbf{T}_{n+1} = \mathbf{T}^{tr} - \mathbf{C}^e : \Delta\gamma\mathbf{N}_{n+1}$ (See Table 1.)
5.	Calculate consistent tangent modulus $\mathbf{C}_{n+1}^k$ $\mathbf{C}_{n+1}^k = K\mathbf{1}\otimes\mathbf{1} + \frac{\partial\mathbf{s}_{n+1}^k}{\partial\Delta\mathbf{E}_{n+1}^Q}$
6.	Update state variables r_{n+1}, $\mathbf{e}_{n+1}^p$ and $\boldsymbol{\beta}_{n+1}$ $\mathbf{e}_{n+1}^p = \mathbf{e}_n^p + \Delta\gamma\mathbf{N}_{n+1}$

Equations (40), (44) and (45) include three independent terms of $\mathbf{s}', \Delta\gamma'$ and r'. Thus, we can find $\mathbf{s}'$ solving those equations and obtain $\partial\mathbf{s}_{n+1}^k / \partial\Delta\mathbf{E}_{n+1}^Q$ in the consistent tangent moduli of equation (41) by the following explicit form.

$$\frac{\partial\mathbf{s}}{\partial\Delta\mathbf{E}_{n+1}^Q} = 2G\hat{\mathbf{E}}^{-1}(\mathbf{I} - \tfrac{1}{3}\mathbf{1}\otimes\mathbf{1}) \tag{46}$$

$$\hat{\mathbf{E}} = a_1\mathbf{I} + \mathbf{a}_2\otimes\mathbf{c}_4 + \mathbf{a}_3\otimes\mathbf{b}_4 \tag{47}$$

Details for a_1, $\mathbf{a}_2$, $\mathbf{a}_3$, $\mathbf{c}_4$ and $\mathbf{b}_4$ are described in Appendix II. Table 2 shows the algorithm of constitutive routine coded in UMAT of ABAQUS.

5. Example

The example problem is a full-scale embankment built rapidly to failure on soft Malaysian marine clay, which was performed by Malaysian Highway Authority (MHA 1989). The embankment was compacted in 0.2m at a nominal rate of 0.4m per week. The width of the embankment was 40m at bottom, the height was 5.4m and the length was 60m.

The nonlinear FE analysis was performed for a mesh

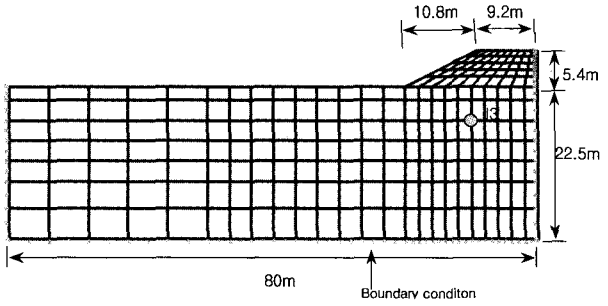

Fig. 2. Finite element mesh

consisting of 8-node quadrilateral equation (serendipity) elements under plain strain condition, as shown in Fig. 2. Elements of the subsoil (soft clay) were created without initial stresses and then those of the embankment were created, in which body forces are governed by load-time functions.

The trial embankment was controlled and monitored carefully by MHA (1989), and the material properties were also evaluated sufficiently. The embankment was modeled by the Drucker-Prager model in this study, and the parameter values are as follows (Brand 1991); E=5100 kPa, n=0.3, ν=0.3, γ =20.5kN/m^3, c=30kPa and ϕ=37°.

For clays the analyses were performed incorporating two constitutive models; i.e., the proposed model and Mises model. The undrained shear strengths of clays are listed in Table 3, which have been evaluated from vane tests by MHA. According to the undrained strengths clays were decomposed in 6 layers in the analysis. Poisson's ratio is assumed to be equal to 0.4999 for simulating undrained condition.

For Mises model, secant Young's moduli were evaluated from laboratory tests by MHA as shown in Table 3. A deviatoric stress invariant is defined as $q = \sqrt{3/2}\|\mathbf{s}\|$ or $q = \sigma_1 - \sigma_3$ in triaxial tests. q_{max} is q at maximum or at failure and

$$q_{max} = 2s_u \tag{48}$$

where s_u is undrained strength for each layer.

For the proposed model the radius of bounding surface for each layer was also defined for each layer as follows

Table 3. Parameter values of constitutive models for clays

Depth (m)	Undrained strength (kPa)	q_{max}[1] (kPa)	Poisson's ratio[1]	Secant moduli[2] (kPa)	Initial moduli[3] (kPa)	a [3]	b [3]	c [3]
0 ~2	25	50	0.4999	25500	98000	0.0122	2.0714	0.3
2 ~5	11.5	23		6600				
5 ~8	14	28		8933				
8 ~11	18	36		9120				
11~14	24	48		6593				
14~	32	64		5884				

[1] For both models
[2] For Mises model
[3] For the proposed model

$$R = \sqrt{\frac{2}{3}} q_{\max} \tag{49}$$

In both Mises and the proposed models maximum stresses or strengths were evaluated from undrained strengths for each layer.

Hardening parameters for the proposed model were interpreted from the results of unconsolidated undrained triaxial tests results by Dangole (1989) as shown in Table 3. The Young's modulus was obtained from the initial tangent which is about 98,000kPa in this example. However, the accuracy of the initial (or maximum) Young's moduli is not so important because the parameter a can also control the initial portion of the stress-strain relationship.

As a result, Fig. 3 shows relationships between deviatoric stress (q) and axial strain in clay layers. Mises model is bilnear while the proposed model, named by GUX for simplicity, is fully nonliear.

In order to verify the accuracy of the algorithm of implicit stress integration, the embankment of 5.4m height was filled at once in large deformation analyses and the body force was controlled by load-time functions. The numbers of increments were 6, 13 and 24 in case 1, case 2 and case 3.

As a result, Fig. 4 shows the nonlinear relationships of load (time step)-displacement in which vertical displacements appear at the center of the embankment and horizontal displacements at the point I3 in Fig. 2. Comparing calculations with case 3 of the smallest increment loading, errors are insignificant and differences are not observable. The values of displacements at the end are shown in Table 4, which shows nearly identical displacements for all cases. Accordingly, it was found that

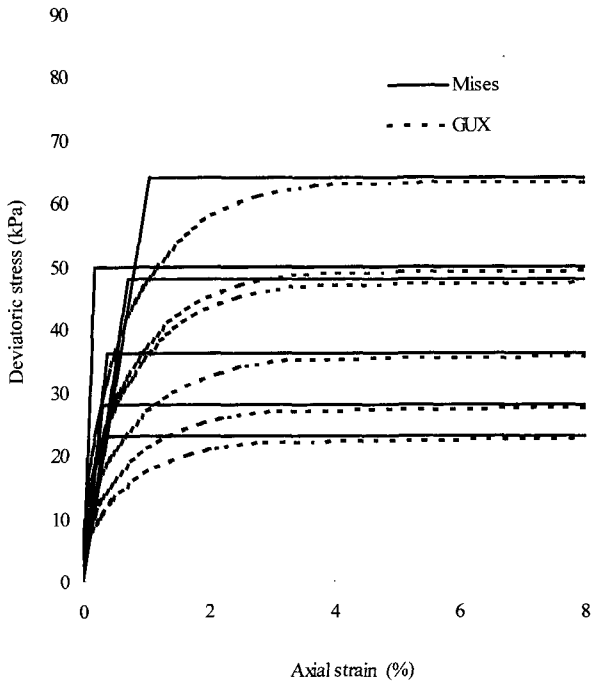

Fig. 3. Stress-strain relationships

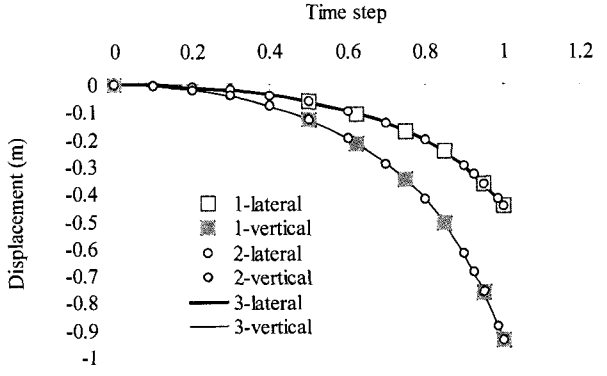

Fig. 4. Fill thickness-displacement curves for various loading steps

Table 4. Displacements and average numbers of iteration

Method #	# of increments	Vertical displacement (cm)	Horizontal displacement (cm)	Average # of iterations/increment	CPU time(sec)
1	6	9.38	4.44	5.3	11.1
2	13	9.35	4.44	3.7	13.4
3	24	9.35	4.44	2.8	18.9

the numerical integration was performed accurately.

The rate of convergence was so rapid that solutions converged within 2 to 6 iterations. The convergence rate was asymptotically quadratic, since the consistent tangent moduli conserved the efficiency of Newton's method.

From the analysis results of accuracy and convergence rate, it was found that the proposed constitutive model was formulated and coded accurately and efficiently, which made the nonlinear analysis of field problems possible.

The actual embankment was analyzed and parameters of soft clays are shown in Table 3. Jeon et al. (2002) already showed that finite strain analyses considering geometric nonlinearity calculated smaller displacement than infinitesimal strain ones which included errors in the mathematical formulation. For infinitesimal strain assumption the displacement occurs rapidly near maximum fill height which might be underestimated.

Fig. 5 shows the simulation of unloading after 3.5m fill. The final heave after full unloading is around 0.1m and Mises model indicates larger value than the proposed model. The process of unloading and reloading is linearly simulated in Mises model while the proposed model could simulate nonlinear relationship in that process.

6. Conclusions

In order to implement an anisotropic hardening constitutive model for soils into ABAQUS code, the formulation included (1) a constitutive equation with Jaumann rate in the rotated frame by Hughes-Winget tensor, (2) implicit stress integration procedure and (3) consistent tangent moduli. The formulation was coded to a user subroutine UMAT in ABAQUS and it made possible to perform large deformation analyses with the proposed constitutive model.

It was verified that the stress integration algorithm was accurate and that the consistent tangent modulus conserved the quadratic rate of convergence. The accurate and efficient algorithm allows analysis of field problems using the anisotropic hardening constitutive model. In the large deformation analysis of a test embankment, the proposed model could simulate the nonlinearity of unloading and reloading sequences.

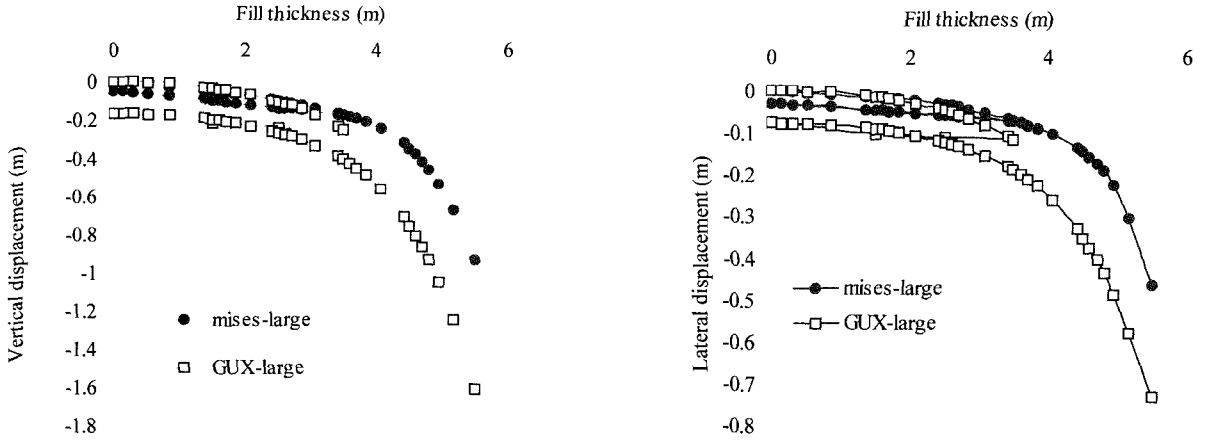

(a) Vertical displacement at the center

(b) Horizontal displacements at I3

Fig. 5. Displacements with unloading and reloading.

Acknowledgement

This research was supported by Korea Science and Engineering Foundation through grant No. R01-2001-000-00482-0. The financial support is gratefully acknowledged.

References

1. Brand, E. W. (1991). Predicted and observed performance of an embankment built to failure on soft clay, *Geotechnical Engineering*, 22, 23-41.
2. Borja, R.I. and Amies, A. P. (1994). Multiaxial Cyclic Plasticity Model for Clays, *J. Geotechnical Engineering Div.*, ASCE, 120, 1051-1070.
3. Crisfield, M. A. (1991). *Non-linear Finite Element Analysis of Solids and Structures, Vol. 1: Essentials*, John Wiley & Sons.
4. Dafalias, Y. F. (1981). The Concept and Application of Bounding Surface in Plasticity Theory, in J. Hult and J. Lemaitre(eds.), *Physical Non-Linearities in Structural Analysis*, IUTAM Symposium, Senlis, France, 1980, Springer Verlag, Berlin, Germany, 56-63
5. Dangole, B. M. S. (1989). Evaluation of geotechnical parameters for settlement and stability analysis of a highway embankment on soft Muar clay, *MEng Thesis*, AIT.
6. Dodds, R. H. (1987). Numerical techniques for plasticity computations in finite element analysis, *Computers & Structures*, 26, 767-779.
7. HK & S, Hibbitt, Karlsson & Sorensen, Inc. (2001) *ABAQUS/ Standard Users Manual*, version 6.2
8. Hughes, T. J. R. (1984). Numerical Implementation of Constitutive Models: Rate-Independent Deviatoric Plasticity, in Nemat-Nasser, S., Asaro, R.J. and Hegemier, G. A. (Eds.), *Theoretical Foundation for Large-Scale Computation of Nonlinear Material Behavior*, Martinus Nijhoff Publishers, Boston, 29-57
9. Hughes, T. J. R. and Winget, J. (1980). Finite Rotation Effects in Numerical Implementation of Rate Constitutive Equations Arising in Large Deformation Analysis, *Int. J. for Numerical Method in Engineering*, 15, 1862-1867
10. Jeon, B.-G., Han, S.-S. and Oh, S. (2002) Large deformation analysis using an anistropic hardening constitutive model: II. Analysis, *J. of Korean Geotechnical Society*, 18, 215-228
11. Lee, S. R. and Oh, S. (1995). An anisotropic hardening constitutive model based on generalized isotropic hardening rule for modeling clay behavior, *Int. J. Numerical and Analytical Methods in Geomechanics*, Vol. 19, pp.683-703.
12. Lush, A. M., Weber, G. and Anand, L., (1989). An Implicit Time-Integration Procedure for a Set of Internal Variable Constitutive Equations for Isotropic Elasto-Viscoplasticity, International Journal of Plasticity, 5, 521-549
13. Lush, A. M. (1990). *Computational Procedures for Finite Element Analysis of Hot-Working*, Ph.D Thesis, Department of Mechanical Engineering, MIT, Cambridge, MA.
14. MHA, Malaysian Highway Authority. (1989). *Proceedings of the International Symposium on Trial Embankments on Malaysian Marine clays*, Kuala Lumpur, 1.
15. Mroz, Z., Norris, V.A. and Zienkiewicz O.C. (1981). An anisotropic critical state model for soils subject to cyclic loading, *Geotechnique*, Vol. 31, pp.451-469.
16. Oh, S. and Lee, S. R. (2001). Formulation of implicit stress integration and consistent tangent modulus for an anisotropic hardening constitutive model, *Computer Methods in Applied Mechanics and Engineering*, 191, 255-272.
17. Oh, S. (2003). An elasto-plastic constitutive model based on anisotropic hardening rule for the soil behavior in overall strain ranges, *Int. J. Numerical and Analytical Methods in Geomechanics*, submitted
18. Ortiz, M. and Popov, E. P. (1985). Accuracy and stability of integration algorithms for elastoplastic constitutive equations, *Internat. J. Numer. Methods Engrg.*, 21, 1561-1576.
19. Simo, J. C. and Hughes, T. J. R. (1998). *Computational Inelasticity*, Springer
20. Simo, J. C. and Taylor, R. L. (1985). Consistent tangent operators for rate-independent elastoplasticity, *Computer Methods in Applied Mechanics and Engineering*,48, 101-118.

Appendix I. Jacobian matrix for stress integrations

The derivatives of yield function with respect to stresses and internal variables are derived from equation (6) as follows.

$$\mathbf{N} \equiv \mathbf{N}_{n+1} = f_{,\mathbf{s}} = -f_{,\boldsymbol{\beta}} = 2(\mathbf{s}-\boldsymbol{\beta}) \tag{A1.1}$$

$$f_{,r} = -2r \tag{A1.2}$$

From the geometry characteristics shown in Fig. 1

$$\frac{\partial \boldsymbol{\beta}}{\partial r} = \frac{\mathbf{b}-\boldsymbol{\eta}}{R} \tag{A1.3}$$

The Jacobian components for residual vector $\mathbf{R}$ are derived from equation (36) as follows.

I.1 Derivatives of r_1

$$\mathbf{r}_{1,\mathbf{s}} = \mathbf{I} + 2G\Delta\gamma\frac{\partial \mathbf{N}}{\partial \mathbf{s}}, \mathbf{r}_{1,\Delta\gamma} = 2G\mathbf{N}, \mathbf{r}_{1,r} = 2G\Delta\gamma\frac{\partial \mathbf{N}}{\partial r} \tag{A1.4}$$

$$\frac{\partial \mathbf{N}}{\partial \mathbf{s}} = 2\mathbf{I}, \frac{\partial \mathbf{N}}{\partial r} = -2\boldsymbol{\beta}_{,r} \tag{A1.5}$$

I.2 Derivatives of r_2

$$r_{2,\mathbf{s}} = \sqrt{\frac{2}{3}}\frac{\partial \|\mathbf{e}^p\|}{\partial \mathbf{s}}, r_{2,\Delta\gamma} = \sqrt{\frac{2}{3}}\frac{\partial \|\mathbf{e}^p\|}{\partial \Delta\gamma}, r_{2,r} = \sqrt{\frac{2}{3}}\frac{\partial \|\mathbf{e}^p\|}{\partial r} - \psi_{,r} \tag{A1.6}$$

$$\frac{\partial\|\mathbf{e}^p\|}{\partial\mathbf{s}} = \frac{\mathbf{e}^p}{\|\mathbf{e}^p\|} : \frac{\partial\mathbf{e}^p}{\partial\mathbf{s}}, \frac{\partial\mathbf{e}^p}{\partial\mathbf{s}} = \Delta\gamma\frac{\partial\mathbf{N}}{\partial\mathbf{s}} \quad \text{(A1.7)}$$

$$\frac{\partial\|\mathbf{e}^p\|}{\partial r} = \frac{\mathbf{e}^p}{\|\mathbf{e}^p\|} : \frac{\partial\mathbf{e}^p}{\partial\Delta\gamma}, \frac{\partial\mathbf{e}^p}{\partial\Delta\gamma} = \mathbf{N} \quad \text{(A1.8)}$$

$$\frac{\partial\|\mathbf{e}^p\|}{\partial r} = \frac{\mathbf{e}^p}{\|\mathbf{e}^p\|} : \frac{\partial\mathbf{e}^p}{\partial r}, \frac{\partial\mathbf{e}^p}{\partial r} = \Delta\gamma\frac{\partial\mathbf{N}}{\partial r} \quad \text{(A1.9)}$$

From equation (6),

$$\frac{\partial\psi}{\partial r} = \frac{ab(r/R)^{b-1} + c(1-r/R)^{c-1}\psi}{R(1-r/R)^c} \quad \text{(A1.10)}$$

I.3 Derivatives of r_3

$$r_{3,\mathbf{s}} = \mathbf{N}, r_{3,\Delta\gamma} = 0, r_{3,r} = f_{,\beta} : \beta_{,r} + f_{,r} \quad \text{(A1.11)}$$

Appendix II. Consistent tangent moduli

From equation (40), we obtain

$$a_1\mathbf{s}' + \mathbf{a}_2 \otimes r' + \mathbf{a}_3 \otimes \Delta\gamma' = 2G(\mathbf{I} - \tfrac{1}{3}\mathbf{1}\otimes\mathbf{1}) \quad \text{(A2.1)}$$

where

$$a_0 = 4G(\Delta\gamma), a_1 = 1 + a_0, \mathbf{a}_2 = -a_0\beta_{,r}, \mathbf{a}_3 = 2G\mathbf{N} \quad \text{(A2.2)}$$

Equation (44) is written as

$$\mathbf{b}_1 : \mathbf{s}' + b_2 r' + b_3\Delta\gamma' = 0 \quad \text{(A2.3)}$$

where

$$b_0 = \frac{2\sqrt{2/3}\Delta\phi}{\|\mathbf{e}^p\|}, \quad \mathbf{b}_1 = b_0\mathbf{e}^p,$$

$$b_2 = -\psi_{,r} - b_0\mathbf{e}^p : \beta_{,r}, b_3 = \sqrt{\tfrac{2}{3}}\frac{\mathbf{e}^p}{\|\mathbf{e}^p\|} : \mathbf{N} \quad \text{(A2.4)}$$

From equation (45)

$$\mathbf{c}_1 : \mathbf{s}' + c_2 r' = 0 \quad \text{(A2.5)}$$

where

$$\mathbf{c}_1 = \mathbf{N}, c_2 = f_{,\beta} : \beta_{,r} + f_{,r} \quad \text{(A2.6)}$$

Equation (A2.5) yields

$$\frac{\partial r}{\partial\Delta\mathbf{E}^Q_{n+1}} = \mathbf{c}_4 : \frac{\partial\mathbf{s}}{\partial\Delta\mathbf{E}^Q_{n+1}} \quad \text{(A2.7)}$$

where $\mathbf{c}_4 = -\mathbf{c}_1 / c_2$. By substituting equation (A2.7) for equation (A2.3),

$$\frac{\partial\Delta\gamma}{\partial\Delta\mathbf{E}^Q_{n+1}} = \mathbf{b}_4 : \frac{\partial\mathbf{s}}{\partial\Delta\mathbf{E}^Q_{n+1}} \quad \text{(A2.8)}$$

where $\mathbf{b}_4 = \mathbf{b}_1 / b_3 - b_2\mathbf{c}_4 / b_3$.

Therefore, equation (A2.1) yields the consistent tangent modulus in equation (41)

$$\frac{\partial\mathbf{s}}{\partial\Delta\mathbf{E}^Q_{n+1}} = 2G\hat{\mathbf{E}}^{-1}(\mathbf{I} - \tfrac{1}{3}\mathbf{1}\otimes\mathbf{1}) \quad \text{(46 } bis.\text{)}$$

$$\hat{\mathbf{E}} = a_1\mathbf{I} + \mathbf{a}_2 \otimes \mathbf{c}_4 + \mathbf{a}_3 \otimes \mathbf{b}_4 \quad \text{(47 } bis.\text{)}$$

(received on May. 14, 2003, accepted on Jul. 29, 2003)